Earthquake Engineering, Tenth World Conference © 1992 Balkema, Rotterdam. ISBN 90 5410 060 5

Distinct element simulation for simple shear test of granular assembly

K. Iwashita
Faculty of Engineering, Saitama University, Urawa, Japan
T. Kojima
Nippon Telegram and Telephone Company, Tokyo, Japan

ABSTRACT: Simple shear test of granular assemblies are simulated numerically using the Distinct Element Method. The detail of the simulation is such that represented the laboratory simple shear test of cylinder assemblies performed by Oda and Konishi. And qualitative tendencies, as the rotation of selected directions for contact normals and contact force, are also consistent. Quantitative data such as the gradient of the τ/σ_n curve, the τ/σ_n peak values and volumetric changeness are almost equal to the ones obtained from the test data. It can be concluded that the rotation of the particles dominate the deformation and the sliding does not play an important part. The contact stiffness has an initiate relationship with the macroscopic stiffness of the specimen.

1. INTRODUCTION

Materials, such as soil or sand, are considered as assemblies of independent particles. A numerical simple shear test of a granular assembly is simulated in this study. The Distinct Element Method (DEM), proposed by Cundall(1971), is used as a numerical calculating method. DEM can simulate the assembly deformation before fracture up to the residual states; thus various data, such as coordination number, contact normal and contact force, that are difficult to measure in the laboratory tests can be obtained easily(Iwashita et al.(1990), Casaverde et al.(1989)).

To examine the fracture mechanics of the granular assembly, direct shear test and simple shear test were simulated. The former one is performed as the test run and used to check the outline of the shear deformation. Latter one is to examine the detail. Simple shear test of cylinders which radius smaller than 5mm were performed by numerical simulation in this study. Parameters such as size of the cylinders and apparatus are closely represented in order to simulate the laboratory test performed by Oda and Konishi(1974). But the initial location of the particles is not strictly same. The DEM's parameters are defined from the physical properties, such as Young's modulus, Poisson's ratio and friction coefficient, of the laboratory test. From the simulation, data those are difficult to be got from the laboratory test, as rotation angle of the each particles, coordination number and number of sliding contacts are outputted. Using these data, the process of the mechanics changing is examined in this study.

However, as DEM needs longer CPU time and large storage memory, some techniques are used in order to save computer powers and expenses. These techniques are the following; using larger elements, using fewer elements and using soft contact stiffness. The last technique is often used, as it is possible to save a lot in CPU time. However, it is not well confirmed its influence on the results. That is why the results are regarded as qualitative ones. The low of similarity can also be used, but it is difficult to represent all the parameters and the conditions totally. In this study, the influence of the soft stiffness on the results is discussed.

2. METHOD

An illustration of the test model is shown in Fig. 1. The distribution of particle radius is almost identical but the location of the particles is different. A normal stress σ is applied to the upper frame of the apparatus, and the lower frame is moved constantly in the horizontal direction. Then the specimen is subjected to shear at a constant strain rate condition. The specimen is consolidated in the vertical direction before shear force is applied. Gravity does not work in this study. before the shear test the specimen is preconsolidated with same or half normal stress σ_n of the shear test. Former one becomes dense specimen and latter becomes loose.

The average stress of the specimen $< \sigma_{ij} >$, with a volume V, is calculated from the local microscopic stresses σ_{ij}.

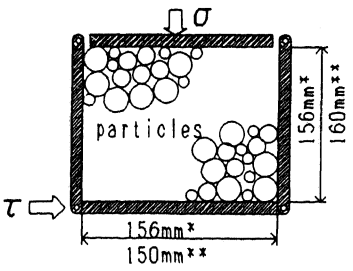

Fig. 1 Shear test model of a two-dimensional granular material. (*laboratory test, **simulation)

Table 1 Parameters of laboratory test (Oda & Konishi) and DEM simulation.

	Laboratory test	Simulation
frame size(net)	width 156mm, height 156±20 mm	width 150mm, height 160± x mm
number of elements	483	456
radius(particles)	3mm(267), 4mm(132), 5mm(84)	3mm(252), 4mm(124), 5mm(80)
elements length	19 mm	19 mm
physical friction angle	18 ~ 25°	0, 10, 24, 45, 84, 89, 89.9°
Young ratio	3.0×10^8 N/m²	1.5×10^6, 3.0×10^6, 3.0×10^8 N/m²
Poisson's ratio	0.2	0.2
normal stress σ_n	1.32×10^5 N/m²	1.32×10^5 N/m²

$$< \sigma_{ij} > = \frac{1}{V}\int_V \sigma_{ij} dV \quad (1)$$

Using the Gauss theory, the equation (1) is transformed in;

$$< \sigma_{ij} > = \frac{1}{2V}\int_S (\sigma_{ik}x_j n_k + \sigma_{jk}x_i n_k) dS \quad (2)$$

in which n_i is the contact normal and x_i is the particle ordinates.

Equation (2) is transformed as follows,

$$< \sigma_{ij} > = \frac{1}{2V}\int_S (f_i x_j + f_j x_i) dS \quad (3)$$

in which $f_i(=\sigma_{ij}n_j)$ is the contact force at the boundary surface. Here, the area of the specimen S equals V when assuming a unit length for the cylinder depth. The average shear stress τ is,

$$\tau = < \sigma_{12} > = \frac{1}{2S}\int_S (f_1 x_2 + f_2 x_1) dS \quad (4)$$

Since this model is an assembly of particles, τ is calculated as follows,

$$\tau = \frac{1}{2S}\sum^{m}(f_1 x_2 + f_2 x_1) \quad (5)$$

where m is the number of the elements in the area S.

The dilatation due to shear deformation is measured by vertical strain = (incremental height ΔH)/(initial height of the specimen H).

The parameters for the laboratory test and the simulation are shown in Table 1. The normal stress σ_n and specimen size is same with the test. The contact stiffness of DEM is calculated from the Young's modulus by Herzian contact theory of elastic cylinders. At the contact between every two particles, Coulomb's friction is considered. Physical friction angle of the laboratory test is 17 ~ 24 ° and one of simulation is changed from 0 to 90 ° . When friction angle is 0 ° , sliding occurs at every contacts and no particles rotates. And the coefficient of the dashpot at the contact of particles are changed and tested.

3. RESULTS

3.1 Comparison of laboratory test and simulation

Fig. 2 shows the relations between stress ratio τ/σ_n and shear distortion γ for laboratory test and DEM simulation (friction angle is 24 ° , dense case). The gradient of the stress ratio curve of the simulation (so-called macroscopic

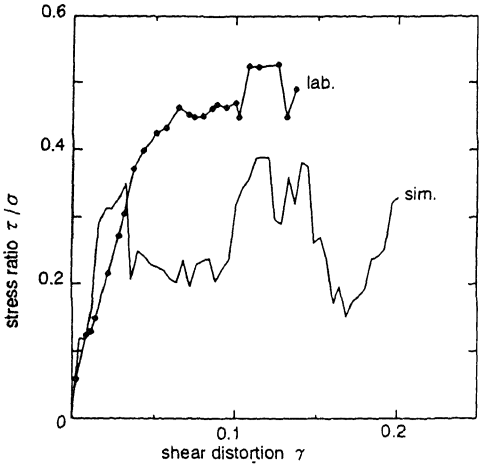

Fig. 2 Relationship between τ/σ_n and γ obtained from two-dimensional simple shear tests for laboratory test and simulation.

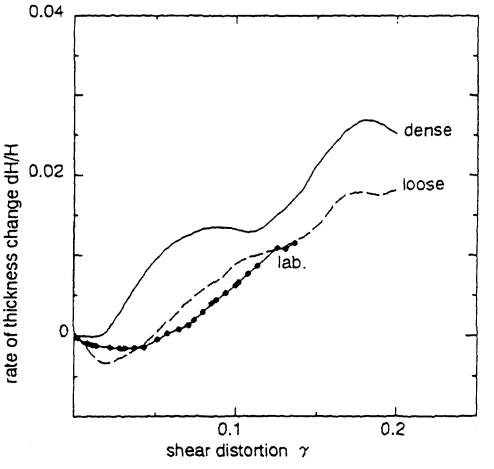

Fig. 3 Relationship between ΔH/H and γ obtained from two-dimensional simple shear tests for laboratory test and simulation.

stiffness) is little bigger than the test. The peak value of τ/σ_n of the simulation is 0.4 and similar to the test value (0.5). The outline of τ/σ_n curve in both cases can be considered similar. In the simulation the curve yields at $\gamma = 5\%$, then softening occurs, while the test does not yield until γ reaches 15%. Then the specimen shows softening and hardening by turns. The results of simulation with other contact stiffness, friction coefficient or damping coefficient yield similarly before γ reaches 10%. All case of simulation use same initial location of particles and it may influence the results. The internal friction angle of the specimen ϕ, which is calculated at the peak point of the τ/σ_n curve, is about 22 ° in the simulation.

Fig. 3 shows rate of thickness change $\Delta H/H$ and shear distortion γ curve. The curve shows negative dilatancy at early shear stage. The line of dense case is obtained from identical case with Fig. 2. However this curve shows only dilatancy from the beginning. This curve shows two peaks and it is consistent with the two times softening of the stress ratio curve in Fig. 2. The dilatancy occurs with the softening of the specimen and negative dilatancy occurs with the hardening.

The line of loose case is obtained from the specimen which was preconsolidated with half level of σ_n of the shear test. So the initial void ratio is looser. This curve shows negative dilatancy at the beginning, then dilatancy occurs. It can be seen consistent with the curve of test. The stress ratio curve of loose case is similar to the dense case, but the peak value is little smaller.

Fig. 4 shows the relationship between the τ/σ_n, γ and m, average coordination number of each particle. At initial stage, one particle contacts with other three particles on average. With the shearing of the specimen, it decreases to nearly two. This line is the average of all the particles. And this specimen is an assemble of cylinders of three radius size. With the larger radius, the particle contacts more. But the period of the changing of m for each three radii is similar, and the the difference of radius does not seem to influence heavily.

The period of changing of m - γ curve coincides with the change of τ/σ_n - γ curves. When m increases, τ/σ_n also increases. Chen and Ishibashi (1990) reported as follows. The shear modulus has a close relationship with the coordination number. During the deformation, the coordination number decreases, the sample becomes less rigid and its shear modulus decreases. Our result agrees with their result.

It may be explained as follows (see Fig. 5); The system of granular assembly can be modeled as the combined system of physical elements. In DEM, each element which is made from spring and dashpot etc., is located at every contact between two particles and it controls the deformation and the movement of the elastic body. Of course, the assembly deforms at next time step, and the physical system is rebuild up to next stage. Then the model which m is large has much physical elements and the combined shear modulus and stiffness , macroscopic stiffness of the system, will be rigid. Conversely m is little, the elements will be few and the total combined stiffness will be soft.

The location of the sliding at the contacts changes rapidly and widely all over the specimen. Sliding does not occur at the same place and does not last too long either. It is difficult to distinguish the deformation stage using the sliding distribution at the contacts as the number of sliding at the contacts is almost constant during

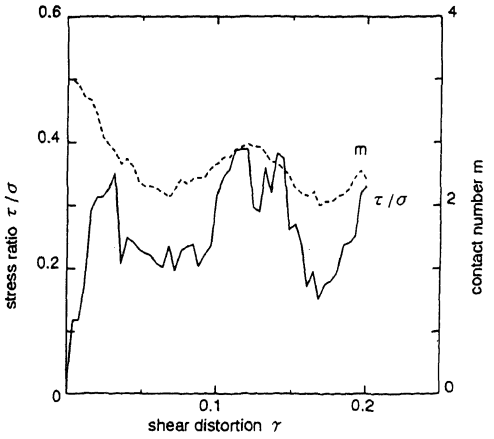

Fig. 4 Relationship between τ/σ_n, γ and m, average number of contacting particles of each particle obtained from simulation.

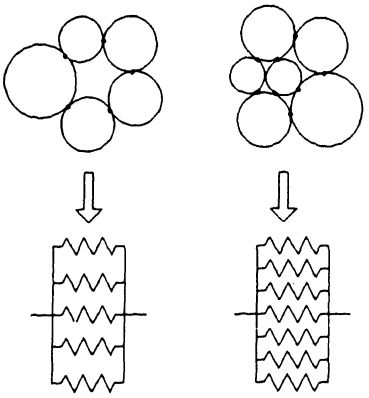

Fig. 5 System of granular assembly and its laugh physical model. (only normal springs are plotted)

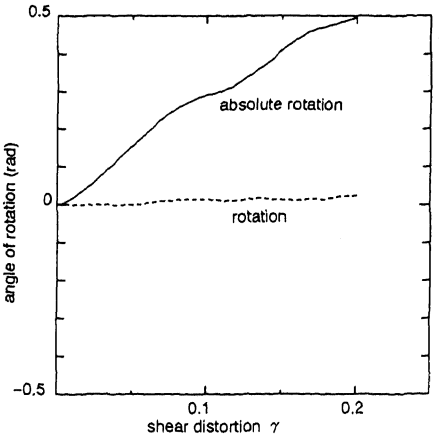

Fig. 6 Relationship between average rotation angle, average absolute rotation angle of particles and γ.

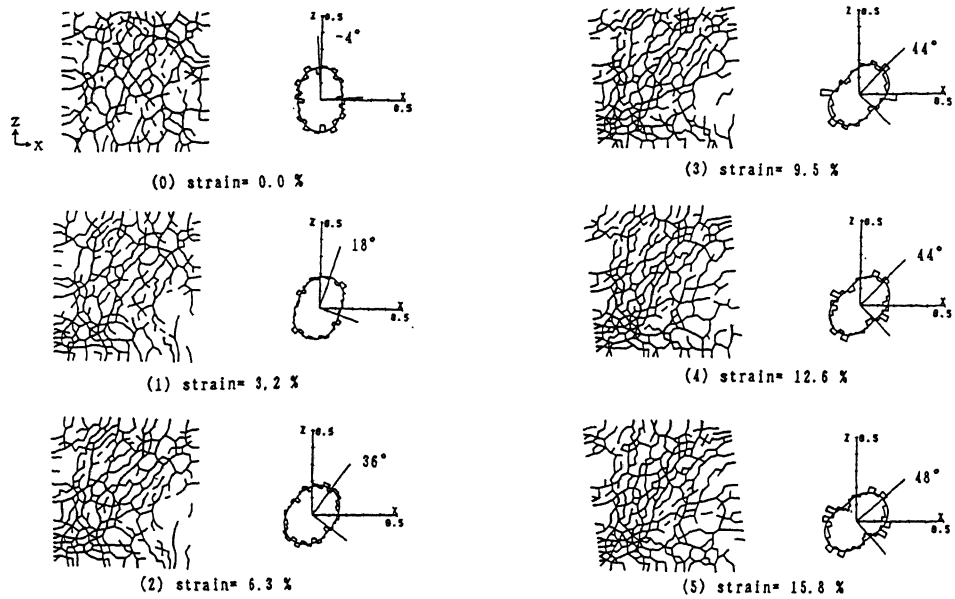

Fig. 7 Directional distribution and frequency distribution of contact force for simulation.

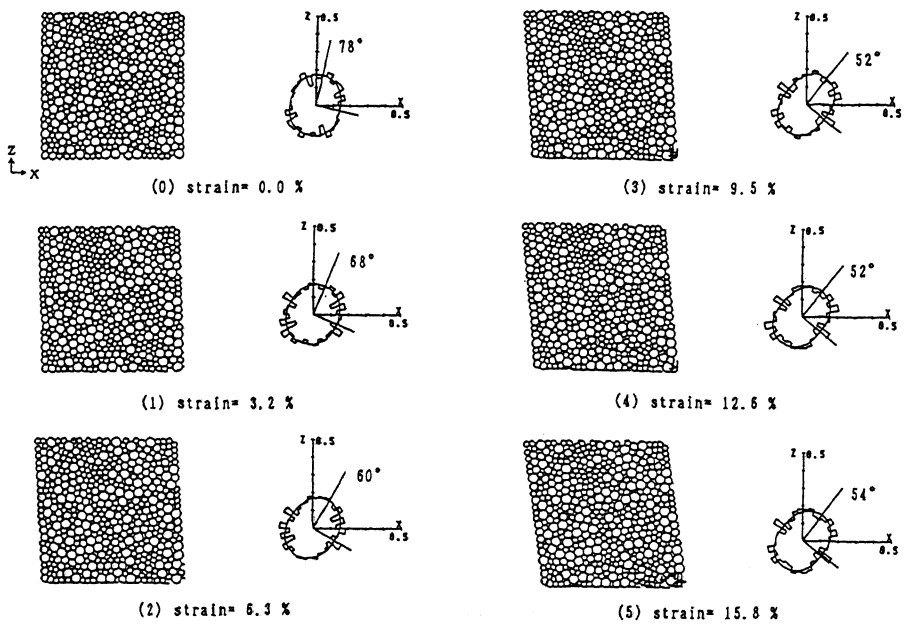

Fig. 8 Sliding distribution sliding at the contact and frequency distribution of contact normal for simulation.

shear deformation. The localization of the strain does not occur until γ reaches 20%.

Fig. 6 shows the relationship between average rotation angle, average absolute rotation angle of particles and γ. When there is no sliding at the contacts and rotation angle of all the particles equilibrates, former keeps zero while latter increases constantly. In this case, the former keeps almost zero constantly, then the equilibrium is satisfied well. The rate of sliding contacts keeps almost constant. If the sliding mainly control the deformation of the granular assembly, the equilibrium of rotation will not be satisfied. Therefore it can be concluded that the rotation of the particles dominate the deformation and the sliding does not play an important part.

Fig. 7 shows the skeleton graph of the contact force and the frequency distribution of the selected direction for the contact force during shear deformation. Fig. 8 shows the distribution of the relative movement and frequency distribution for the contact normal. In the skeleton graph of Fig. 7 it is possible to see that the selected direction of the force is in vertical direction at the first stage. Then it rotates according to the maximum principal stress. And the vertical branches of the contact force disappear while diagonal branches appear in the principal stress direction gradually. At an early stage (about γ = 3%), the main trunk in the diagonal direction is formed from the branches. When the contacts between particles fail, new contacts occur immediately close by so that fracture does not occur in series. Therefore it is not possible to distinguish the fracture of the fabric from the skeleton graph clearly, this can be stated also for the data of sliding at the contact.

3.2 Effect of contact stiffness

The above results are calculated with the contact stiffness which was determined from the real Young's modulus of the material. Fig. 9 shows the $\tau/\sigma n$ curves of simulation which contact stiffness are 1/100 and 1/200 and other conditions are identical. The gradient of the curve becomes soft. The peak τ/σ_n decreases together with the stiffness, the peak τ/σ_n decreases. Using the soft stiffness, the coordination number increases, dilatancy decreases and the particles moves flatly, not horizontally.

Then the process may be explained as follows; For the same compressive force a soft contact stiffness allows large overlappings at the contact between particles, while a hard stiffness allows relatively fewer overlappings. And according to the shear force soft particles can move easier than the hard ones in the horizontal direction. Therefore the contact stiffness has an important influence on the deformation mechanism. Rigid body movement may be simulated well with soft stiffness but the deformation of elastic body, such as stress-strain relationship may not simulated well.

3.3 Effect of physical friction coefficient

Fig. 10 shows the relationship between τ/σ_n and γ with friction angle = 0, 24, 45 ° . Other conditions are same. At case of 0 ° , the relative movement of the particles is only sliding and no rotation occurs. This case shows small τ/σ_n peak than other two cases. The two curves of 24

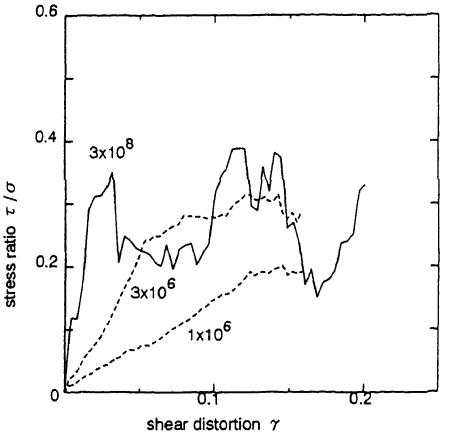

Fig. 9 Relationship between τ/σ_n and γ obtained from simulation with 1/100 and 1/200 times the contact stiffness.

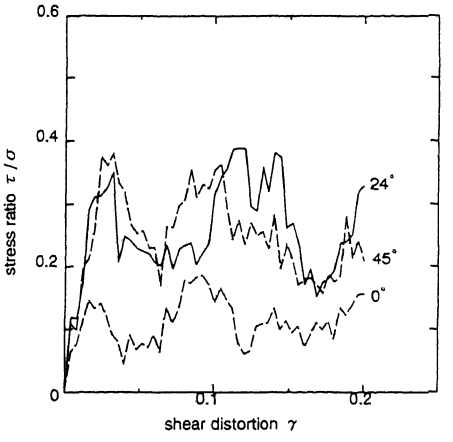

Fig. 10 Relationship between τ/σ_n and γ obtained from the simulation with friction angle = 0, 24, 45 °

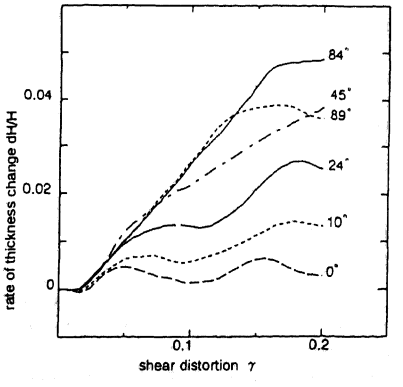

Fig.11 Relationship between $\Delta H/H$ and γ obtained from the simulation with physical friction angle = 0, 10, 24, 45, 84, 89 °

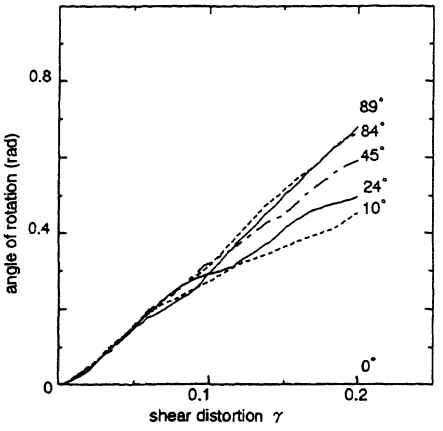

Fig. 12 Relationship between average absolute rotation angle and γ obtained from the simulation with friction angle = 0, 10, 24, 45, 84, 89 °

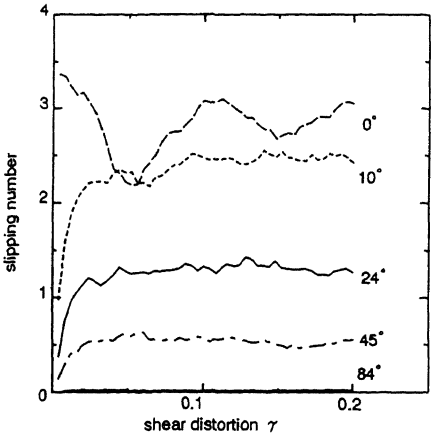

Fig. 13 Relationship between average number of sliding contact and γ obtained from the simulation with friction angle = 10, 24, 45, 84 °

and 45 ° have a same initial gradient and the peaks are not so different.

With friction angle=84 ° , the peak does not rise. From this simulation, the physical friction has less relationship with the internal friction. But further research will be necessary.

Fig.11 shows the relationship between $\Delta H/H$ and γ. With the physical friction angle, the $\Delta H/H$ increases remarkably. There is a limit of $\Delta H/H$ even if the friction angle increases. Particles does not rotate in case of friction angle=0 ° , but $\Delta H/H$ occurs. The curves of small friction angle, as 0, 10, 24 ° , have two peaks. It may owe to the initial location of the sample. In all cases, same particle location is used as the initial sample. It may be necessary to use another initial location. Then the curves will be changed.

Fig. 12 shows the relationship between average rotation angle and γ. The rotation angle increases together with the physical friction angle.

Fig. 13 shows the relationship between average number of sliding contact and γ. As expected, frequency of sliding decreases with the friction. In all cases, the frequency of sliding is almost constant. Therefore it may be concluded that there is no relation between frequency of sliding and deformation stage, as peak and post peak.

For check the effect of dashpot at the contacts, three damping coefficient(2, 5, 10%) are used. And the results are almost identical in all the data. So it can be concluded that the effect of the dashpot coefficient at the contact is not so important. It will be confirmed that the role of dashpot is to secure the numerical calculation.

4. CONCLUSIONS

Qualitative results of the simulation are almost consistent with the test. The selected directions of contact forces and contact normals rotate according to the maximum principal stress axis. Quantitative data such as the gradient of the τ/σ_n curve, the τ/σ_n peak values and volumetric changeness are almost equal to the ones obtained from the test data.

The contact stiffness has an initiate relationship with the macroscopic stiffness of the specimen. The contact stiffness has an important influence on the deformation mechanism. Rigid body movement may be simulated well with soft stiffness but the deformation of elastic body, such as stress-strain relationship may not simulated well.

During the shearing process, the equilibrium of particle rotation over the specimen is satisfied in total. And the sliding frequency at the contact is almost constant during deformation. And there is no relation between frequency of sliding and deformation stage. It can be concluded that the rotation of the particles dominate the deformation and the sliding does not play an important part.

The coordination number has an initiate relationship between the macroscopic stiffness.

It can be concluded that the effect of the dashpot coefficient is not so important in DEM. It will be confirmed that the role of dashpot is to secure the numerical calculation.

REFERENCES

Casaverde, L., Iwashita, K., Tarumi Y., and Hakuno M.: Distinct element analysis for rock avalanche, Proc. of JSCE, No. 404, pp. 153 - 162, 1989.

Chen Y. and Ishibashi I. : Dynamic shear modulus and evolution of fabric of granular materials, Soil and Foundations, Vol. 30, No. 3, pp. 1 - 10, 1990.

Cundall P. A. : A computer model for simulating progressive, Large Scale Movement in Blocky Rocksystem, Symp. ISRM, Nancy, France, Proc., Vol.2, pp. 129 - 136, 1971.

Cundall P. A. and Strack O. D. L. : Modeling of microscopic mechanisms in granular material, Mechanics of Granular Materials, pp. 137 - 149, 1983.

Iwashita, K. and Hakuno, M. : Modified distinct element method simulation of dynamic cliff collapse, Proc. of JSCE, Vol.416, I-13, pp.145 - 154, 1990.

Oda. M and Konishi. J : Microscopic deformation mechanism of granular material in simple shear, Soils and Foundations, Vol.14, No4, pp. 25 - 38, 1974.